

# Digital Image Watermarking using Combined DWT and DFRFT

Farooq Husain  
Deptt. of E & C Engg.  
MIT Moradabad,  
244001, India

Ekram Khan  
Deptt. of Electronics  
Engg  
AMU Aligarh, 202002,  
India

Omar Farooq  
Deptt. of Electronics  
Engg.  
AMU Aligarh, 202002,  
India

## ABSTRACT

In this paper, a digital image watermarking technique combining Discrete Wavelet Transform (DWT) and Discrete Fractional Fourier Transform (DFRFT) has been investigated. This is a non-blind watermarking technique that exploits multi-resolution sub-band decomposition property of DWT and applies DFRFT on selected sub-bands in DWT-transformed image. The performance of this algorithm under various attacks is investigated and compared with DFRFT and DWT-based algorithms. The simulation results show that proposed watermarking technique offers better robustness to all attacks as compared to DWT-based scheme whereas either comparable or better than DFRFT-based technique for all attacks except median filtering, AWGN and JPEG compression attacks.

Keywords -Digital Image Watermarking, Discrete Wavelet Transform, Discrete Fractional Fourier Transform, Histogram Equalization, Sharpening.

## 1. INTRODUCTION

Due to availability of broadband Internet, the use of multimedia based services is increasing day by day and has penetrated in almost every walk of our life. Entertainment, sports, telemedicine, video surveillance are just to mention the few applications of the multimedia. On the other hand, a number of sophisticated tools (Adobe Photoshop, cool audio editor) freely available over the Internet which make copy, manipulation and alteration of multimedia contents so easy that a person with little knowledge of computer and these tools can easily alter the multimedia contents as a fun. In such a scenario, it is very important to have means to authenticate the originality of multimedia contents. Digital watermarking has been proposed as a viable solution to improve multimedia security and to verify the authenticity of the contents while offering the robustness against any attempt to alter contents. Digital watermarking techniques have been used in copyright protection, content authentication, temper proofing, broadcast monitoring and integrity of network [1]-[3]. Digital watermarking techniques can be applied to any multimedia data such as text, audio, image and video.

Image watermarking techniques can be broadly classified in two groups: spatial-domain and transform-domain techniques. The spatial-domain watermarking algorithms [4]-[5] directly embed watermark information into a set of pre-selected pixels of images. These techniques are simple but are not robust enough to various image processing operations. In transform-domain image watermarking, the original image is first transformed into the frequency-domain, and then the transformed coefficients are modified to embed watermark information. Transform-domain watermarking algorithms attract more attention in recent years due to their excellent

robustness against various attacks [10]. The commonly used transforms for watermarking are Discrete Fourier Transform (DFT) [6]-[7], Discrete Cosine Transform (DCT) [8]-[9], Discrete Wavelet Transform (DWT) [10]-[13], and Discrete Fractional Fourier Transform (DFRFT) [14]-[17]. A DFRFT-based watermarking scheme has relatively poor robustness compared to DWT-based watermarking scheme for histogram equalization and sharpening attacks.

Among these transforms, DCT and DWT are probably the most widely used and explored for watermarking applications. However, in recent years, many watermark techniques are developed using DWT due to following reasons; (i) Unlike DCT, DWT is not a block-based transform, and so it does not suffer with annoying blocking artifacts, which is generally associated with the DCT; (ii) The multi-resolution property of DWT, similar to human visual system (HVS), offers more degrees of freedom for embedding. In order to exploit these advantages of DWT, and that of other transforms, a number of watermarking schemes have been developed using either DWT alone [10]-[13], DWT in conjunction with other transforms, such as DCT and DFRFT [16][18]-[21].

The work presented in this paper deals with digital image watermarking using combination of DWT and DFRFT. In the proposed method, host image is first wavelet transformed and then DFRFT is applied to some selected high-frequency sub-bands of transformed image. These DFRFT coefficients are then sorted in the ascending order of their magnitude, and watermark is embedded to first few (equal to watermark length) sorted DFRFT coefficients. The inverse DFRFT and inverse DWT are finally applied to get the watermarked image. A non-blind watermark extraction algorithm has also been developed. The proposed method differs from that of Hong et al. method [16] in the sense that in [16] chirp-type watermark was embedded in the low frequency sub-band (only one), whereas in our method, any watermark data can be embedded in one or many high-frequency sub-bands. Therefore our method is more flexible

Rest of the paper is organized as follows. An overview of DWT and DFRFT is given in section-2. In section-3, watermark embedding and extraction algorithms are discussed. Various simulation results and related discussion are presented in section-4. The paper is finally concluded in section-5.

## 2. OVERVIEW OF DWT AND DFRFT

Discrete Wavelet Transform (DWT) is used to analyze a signal at different frequency bands with different resolutions by decomposing the signal into a coarse approximation and detail information [22]. 1D-DWT employs two sets of functions, called scaling functions and wavelet functions, which are associated with low-pass and high-pass filters, respectively. The decomposition of the signal into different frequency bands is simply obtained by successive high-pass and low-pass filtering

of the time-domain signal. The process of single stage of DWT for 1D-signal is as follows: The original signal  $x[n]$  is first passed through a half band high-pass filter  $g[n]$  and a low-pass filter  $h[n]$ . After the filtering, half of the samples of signal  $x[n]$  can be eliminated according to the Nyquist's criteria, since the signal now has a highest frequency of  $\pi/2$  radians instead of  $\pi$ . The signal can therefore be sub-sampled by 2, simply by discarding every other sample [23]. This constitutes one level of decomposition and can mathematically be expressed as follows:

$$\begin{aligned} y_{high}[k] &= \sum_n x[n] \otimes g[2k-n] \\ y_{low}[k] &= \sum_n x[n] \otimes h[2k-n] \end{aligned} \quad (1)$$

where,  $y_{high}[k]$  and  $y_{low}[k]$  are the outputs of the high-pass and low-pass filters, respectively, after sub-sampling by 2. Symbol  $\otimes$  denotes convolution operation between two signals. At every decomposition level, the filtering and sub-sampling will result in half the time resolution and double the frequency resolution [24].

Since DWT is a separable transform, 1D-DWT can easily be extended to 2D-DWT, by applying 1D transform first by row-wise and then by column-wise. A 2D-DWT applied to an image once decomposes the image into four sub-bands known as LL, HL, LH and HH sub-bands. LL is called approximation band which possesses low frequency coefficients and HL1, LH1 and HH1 are detailed bands containing horizontal, vertical and diagonal edges (high-frequencies) of the image. In dyadic DWT, the same process is repeated on LL sub-band to decompose images into  $(3n+1)$  sub-bands, where  $n$  is the number of decomposition levels. For example, two-level wavelet decomposition and corresponding sub-bands are shown in Figure 1.

LL2 1	HL2 2	HL1 5
LH2 3	HH2 4	
LH1 6		HH1 7

**Figure 1: Different sub-bands of an image for two-level DWT decomposition.**

DWT has been used in digital image watermarking more frequently due to its excellent spatial localization property and multi-resolution characteristics. A major advantage of the DWT lies in the fact that it performs an analysis similar to that of the Human Visual System (HVS), as it also split the image into several frequency bands, similar to HVS.

Fractional Fourier Transform (FRFT) is the generalized form of classical Fourier Transform (FT). FRFT maps a one-dimensional time signal into a two-dimensional function of time and frequency. The FT corresponds to a rotation in the time-frequency plane over an angle equal to  $\pi/2$ . The FRFT corresponds to a rotation over some arbitrary angle  $p\pi/2$  where  $p$  is a floating point number and is known as power or order of FRFT.

The  $p^{\text{th}}$  order continuous FRFT of an analog signal  $f(t)$  is defined as; [25]

$$F^p[f(t)] = \int_{-\infty}^{\infty} K_p(t, u) f(u) du, \quad 0 \leq |p| \leq 2$$

(2)

Where,  $K_p(t, u)$  is the kernel function of the FRFT and it is given as:

$$K_p(t, u) = \begin{cases} \sqrt{\frac{1-j \cot \alpha}{2\pi}} \exp\left(j \frac{t^2 + u^2}{2} \cot \alpha - j \frac{tu}{\sin \alpha}\right), & \text{if } \alpha \neq n\pi \\ \delta(u-t), & \text{if } \alpha = 2n\pi \\ \delta(u+t), & \text{if } \alpha = (2n+1)\pi \end{cases}$$

(3)

and  $p$  is the order of FRFT,  $\alpha$  is the angle of rotation and  $n$  is an integer. The parameters  $p$  and  $\alpha$  are related as  $\alpha = p\pi/2$ .

The inverse of a  $p$ th order FRFT is simply the FRFT with order  $-p$ . That is,

$$f(t) = F^{-p}[F^p(f(t))]$$

(4)

The 2D-DFRFT of an image  $I(x, y)$  is determined as

$$F_{\alpha_1, \alpha_2}(m, n) = \sum_{x=0}^{M-1} \sum_{y=0}^{N-1} I(x, y) K_{\alpha_1, \alpha_2}(x, y, m, n)$$

(5)

The inverse 2D-DFRFT of the transformed image  $F_{\alpha_1, \alpha_2}(m, n)$  is determined as

$$I(x, y) = \sum_{m=0}^{M-1} \sum_{n=0}^{N-1} F_{\alpha_1, \alpha_2}(m, n) K_{-\alpha_1, -\alpha_2}(x, y, m, n)$$

(6)

where,  $K_{\alpha_1, \alpha_2}(x, y, m, n) = K_{\alpha_1} \otimes K_{\alpha_2}$  is the 2D-DFRFT kernel,  $K_{\alpha_1}$  and  $K_{\alpha_2}$  are the 1D-DFRFT kernels. Symbol  $\otimes$  denotes the convolution between  $K_{\alpha_1}$  and  $K_{\alpha_2}$ . Here,

$\alpha_1 = p_1\pi/2$  and  $\alpha_2 = p_2\pi/2$  are the fractional angles of 2D-DFRFT, and  $p_1$  and  $p_2$  are the order or powers of 2D-DFRFT. An FRFT transformation domain is a combination of the time and frequency domains. If  $p_1$  and  $p_2$  are close to 1, the FRFT transformation being dominantly in the frequency domain. On the hand, if  $p_1$  and  $p_2$  are close to 0, FRFT is dominantly in the time domain. For the watermarking proposed in this chapter, a frequency domain dominant case is used. One of the advantage of using DFRFT as a transformation tool for watermark embedding is that by using varying powers of DFRFT, multiple watermarks can be embedded in comparison to other image watermarking techniques such as those based on DFT and DCT. Therefore, higher embedding capacity can be achieved in DFRFT-based image watermarking.

### 3. PROPOSED WATERMARKING TECHNIQUE

In this section, proposed watermark embedding and corresponding extraction algorithms are described.

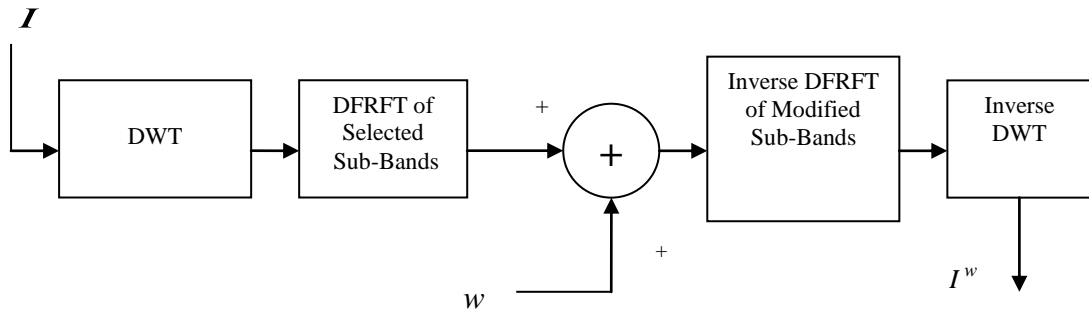


Figure 2: Block diagram of watermark embedding for proposed image watermarking.

### 3.1 Embedding Algorithm

In this scheme, two-level DWT decomposition of a gray scale host image ( $I$ ) is performed using Haar filters. The watermark data is embedded in selected HF sub-bands, i.e. in the one or two sub-bands selected among LH1, HL1, HH1, LH2, HL2 and HH2. The criterion to select the sub-bands is the perceptibility of watermarked image. Each of the selected HF sub-bands is further

transformed using DFRFT and then the transformed coefficients are concatenated in a single one-dimensional array (using raster scan). The DFRFT coefficients of concatenated array are sorted in ascending order of their magnitudes. Some of these coefficients (equal to the watermark length) in contiguous order are selected for watermark embedding and the watermark is added in these coefficients. These watermarked and remaining DFRFT coefficients of sorted array are then placed at their original locations which are finally placed back in HF sub-bands of which they belong. The inverse DFRFT is applied to the selected HF sub-bands, which were earlier transformed using DFRFT. Then inverse DWT is performed to obtain the watermarked image ( $I^w$ ). The block diagram of watermark embedding described above is depicted in Figure 2.

The watermark embedding process can be summarized in the following steps:

- In watermark embedding process, first a  $n$ -levels DWT decomposition of the host image ( $I$ ) is performed which results into  $(3n+1)$  sub-bands, one approximation sub-band ( $LL_n$ ) and  $3n$  detailed sub-bands

$$\left( \sum_i (LH_i + HL_i + HH_i) \right). \text{ That is;}$$

$$X_{wT}^n = \text{DWT}(I) = LL_n + LH_n + HL_n + HH_n + LH_{n-1} + HL_{n-1} + HH_{n-1} + \dots + LH_1 + HL_1 + HH_1 = \sum_{i=1}^{3n+1} sb^i \quad (7)$$

where,  $n$  is the number of DWT decomposition levels (here  $n = 1$  or  $2$ ).  $sb^i$  represents a  $i^{\text{th}}$  sub-band. Different sub-bands along with their indexes for two-level decomposition ( $n=2$ ) of an image are shown in Figure 1.

- Select a set of sub-bands from the detailed sub-bands (HF sub-bands), say this set is  $s^i$ , where  $i$  may have any value from 2 to 7 (refer Figure 1). Perform DFRFT of each HF sub-bands of set  $s^i$  and store DFRFT coefficients in an array  $R$  as defined in Eqn (8).

$$R = F[s^i] \quad (8)$$

where,  $F$  denotes DFRFT transformation operator .

- Sort the elements of set  $R$  in ascending order of their magnitudes and store the sorted data in an array  $Z_s$  .
- Select first 'M' DFRFT coefficients of  $Z_s$  , where  $M$  is the length of watermark data to be embedded. Let  $k^{\text{th}}$  element of  $Z_s$  is  $Z_s[k]$  , where  $k=1, 2, \dots, M$ .
- Add watermark data  $w[k]$  to  $Z_s[k]$  to get watermarked DFRFT coefficients  $Z_s^w[k]$  .

$$Z_s^w[k] = Z_s[k] + w[k], \quad 1 \leq k \leq M \quad (9)$$

$$\text{where, } w[k] = \begin{cases} \alpha, & \text{if watermark bit} = 1 \\ 0, & \text{otherwise} \end{cases}$$

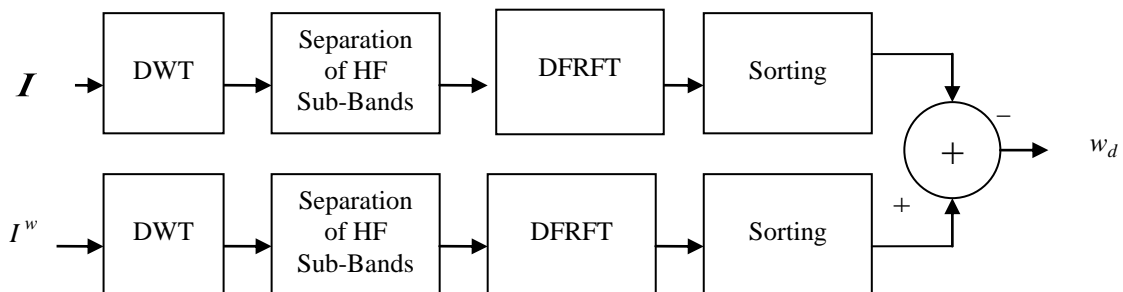


Figure 3 Block diagram of watermark extraction for proposed image watermarking

- These watermarked and remaining DFRFT coefficients of sorted array are then placed at their original locations

which are finally placed back in corresponding HF sub-bands of which they belong.

- Take inverse DFRFT of each modified sub-bands obtained in the previous step.
- Perform inverse DWT to obtain a watermarked image ( $I^w$ ).

### 3.2 Extraction Algorithm

It is basically a non-blind approach in which the knowledge of the original host image is required. Additionally, the watermark extraction process also requires information such as number of DWT decomposition levels, powers of DFRFT transform and index of sub-bands in which watermark was embedded etc. These additional informations may be sent as headers in the watermarked image. The block diagram of the proposed watermark extraction scheme is shown in Figure 3. In order to elaborate the step-by-step watermark extraction procedure, let  $I$  and  $I^w$  represent the host and the received watermarked images respectively. The steps involved in extraction are as follows:

- The first step in the watermark extraction process is to apply one or two levels of 2D-DWT on both  $I$  and  $I^w$ .
- Using the index of HF sub-band from the header, perform DFRFT of HF sub-bands (in which watermark was embedded) for both host and watermarked images.
- If  $R$  is an array containing the DFRFT of set of HF sub-bands for original host image ( $I$ ) and  $R^w$  is an array containing the DFRFT of set of HF sub-bands for watermarked image ( $I^w$ ), then sort the elements of sets  $R$  and  $R^w$  in ascending order of their magnitudes and store the sorted data in an arrays  $Z_s$  and  $Z_s^w$ , respectively.
- The watermark is then extracted by performing element-wise subtraction of first  $M$  elements of array  $Z_s$  from  $Z_s^w$  according to Eqn. (10).

$$w_d = Z_s^w[k] - Z_s[k] \text{ for } 1 \leq k \leq M \quad (10)$$

## 4. SIMULATION RESULTS

In this section, simulation results of proposed digital image watermarking scheme are presented and compared with DFRFT-based scheme and DWT-based watermarking scheme proposed by Kundur and Hatzinakos [26].

### 4.1 Performance Metrics

The performance of the proposed image watermarking algorithm is measured in terms of Peak Signal-to-Noise Ratio (PSNR) of watermarked image and Bit Error Rate (BER) in watermark extraction. These parameters are defined as follows:  
**Peak Signal to Noise Ratio (PSNR):** One of the important features of digital watermarking is that the perceptual quality of the watermarked image should not be degraded much as compared to original one. Imperceptibility of watermarked images is evaluated by measuring its PSNR. Imperceptibility may also be checked by visual inspection of watermarked image and comparing with original host image. PSNR is used to measure the objective quality of watermarked images. The value of PSNR is the measure of similarity between watermarked and host images. It is defined as:

$$PSNR = 10 \log_{10} \left( \frac{255^2}{MSE} \right), \text{dB} \quad (11)$$

Where, MSE is the mean square error between host images ( $I$ ) and watermarked images ( $I^w$ ) each of size  $M \times N$ . It is defined as:

$$MSE = \frac{1}{M \times N} \sum_{x=1}^M \sum_{y=1}^N [I(x, y) - I^w(x, y)]^2 \quad (12)$$

where,  $I(x, y)$  and  $I^w(x, y)$  are pixel intensities of host and watermarked images at  $(x, y)$ , respectively.

**Bit Error Rate (BER):** The performance of extraction algorithm is measured in terms of percentage bit error rate (BER) of the extracted watermark data. The BER in watermark extraction is defined as:

$$BER = \frac{N_e}{N} \times 100 \% \quad (13)$$

Where,  $N_e$  is the number of erroneously extracted watermark bits and  $N$  is the total number of watermark bits.

### 4.2 Simulation Parameters

Implementation parameters of all the three watermarking methods (DWT-based method, DFRFT-based method and proposed method) are summarized as follows. In order to evaluate the performance of proposed watermarking method and for comparison with other two methods, five standard 8-bit gray scale images namely *Lena*, *Boats*, *Goldhill*, *Peppers* and *Baboon*, each of size  $512 \times 512$  pixels are considered. Pixels of a binarized image of size  $32 \times 32$  pixels (*fh.bmp*) are taken as watermark data. Therefore, the length of watermark data is  $32 \times 32 = 1024$  (i.e.  $M = 1024$ ). The watermark data are scaled using a scaling factor ( $\alpha$ ) of 44. The scaling factor determines the threshold ( $Th$ ) for the binarization of extracted watermark data, i.e.  $Th = \text{scaling factor} / 2 = 22$ . The remaining parameters for different methods are as follows:

- DWT-based method [26]: ‘Haar’ filter is used for DWT decomposition of an image with four levels and watermark is embedded in high-frequency sub-bands of 4<sup>th</sup> level.
- DFRFT-based method: for this method, watermark location ( $L$ ) = 259000 and DFRFT powers  $p_h = [p_1, p_2] = [0.99, 0.99]$ .
- Proposed (combined DWT and DFRFT-based) method: ‘Haar’ filter is used for DWT decomposition of an image with two levels and watermark is embedded in combination of high-frequency sub-bands of 1<sup>st</sup> and 2<sup>nd</sup> levels. For this method, watermark location ( $L$ ) = 0 and DFRFT powers  $p_h = [p_1, p_2] = [0.99, 0.99]$ .

Using these parameters, the three methods are simulated and their performances under various attacks, measured in terms of BER of extracted watermark data are summarized in Table 1 for ‘Lena’ image. In this table, the first column includes various channel attacks, second and third columns list BER under various attacks for DWT-based and DFRFT-based methods, respectively. The remaining columns in table 1 give BER performance of proposed method with different combinations of high frequency sub-bands considered for watermark embedding, and under various attacks.

### 4.3 Performance Evaluation

#### 4.3.1 Imperceptibility

Our proposed image watermarking scheme is imperceptible because no visual artifacts has been observed in watermarked ‘Lena’ image in comparison to original un-watermarked ‘Lena’ image as shown in Figure 4. PSNR for watermarked ‘Lena’ images for DWT method, DFRFT method and proposed method (combined DWT and DFRFT) are 45.23 dB, 51.26 dB and 51.35 dB, respectively.

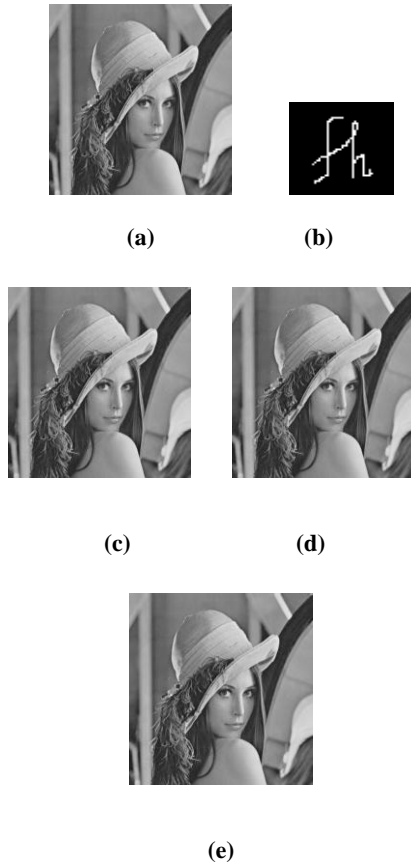


**Figure 4 (a) Original host image ‘Lena’, 512\*512 pixels, gray-scale (b)Watermark image, 32\*32 pixels, binary image (c) Watermarked ‘Lena’ image for proposed(combined DWT and DFRFT) method (d) Watermarked ‘Lena’ image for DWT-based method (e) Watermarked ‘Lena’ image for DFRFT-based method**

#### 4.3.2 Robustness Measurement

Watermark extraction performance under salt & peppers noise, median filtering, Additive White Gaussian Noise (AWGN), JPEG with Quality Factor (QF) of 70%, Low Pass Filtering (LPF), histogram equalization, sharpening for watermark embedded in host image ‘Lena’ is presented in the second to eighth rows of the Table 1 respectively. For the proposed method, its performance is shown for embedding the watermark data in different high frequency sub-bands and their combinations of transformed image. Following observations can be made from the results presented in Table 1:

- For salt & Pepper noise (2<sup>nd</sup> row) and AWGN (4<sup>th</sup> row), proposed method gives lower BER compared to DWT based method, whereas almost comparable BER to that of DFRFT method.
- For median filtering (3<sup>rd</sup> row) and JPEG compression (5<sup>th</sup> row), DFRFT-based method outperforms DWT as well as the proposed method.
- For low pass filtering (6<sup>th</sup> row), histogram equalization (7<sup>th</sup> row) and sharpening (8<sup>th</sup> row), proposed method outperforms the DWT and DFRFT-based method. These are the major advantages of combining DFRFT with DWT based method.

Results of watermark extraction performance for these attacks for images, ‘Lena’, ‘Boats’, ‘Goldhill’, ‘Peppers’ and ‘Baboon’ are illustrated in Figures 5 to 11. In these figures, for proposed method the results of embedding watermark data in HH2 (representative of single HF sub-band), HL1+HH1 (representative of combination of two HF sub-bands of first

level decomposition), HL2+HH2 (representative of combination of two HF sub-bands of second level decomposition) and HL1+HH2 (representative of combination of two HF sub-bands of first level and second level decompositions) sub-bands are presented.

It can be observed from these figures that proposed method outperforms other methods in term of BER for low-pass filtering (Figure 9), histogram equalization (Figure 10) and sharpening (Figure 11) attacks for all images. Further, it can be observed that irrespective of sub-bands in which watermark was embedded, the results are consistently better, compared to other two methods. For other attacks, such as salt and pepper noise (Figure 5), median filtering (Figure 6) and AWGN (Figure 7), BER of proposed method is better than that of DWT for all images under consideration, but it is slightly inferior or comparable to DFRFT based method.

However, for JPEG compression (Figure 8), the proposed method offers highest BER in comparison to other two methods. The reason for this is that since in proposed method, watermark data are embedded in a set of HF sub-bands and when watermarked image is subjected to JPEG compression, high frequency components are distorted, therefore increasing the BER.

## 5. CONCLUSION

It has been observed that DFRFT-based image watermarking scheme shows relatively poor robustness compared to DWT-based watermarking scheme for sharpening and histogram equalization attacks. In order to reduce BER in extracted watermark, a watermarking scheme in combined DWT and DFRFT domains has been developed and its performance has been evaluated. This proposed scheme improves the watermark extraction performance for low-pass filtering, sharpening and histogram equalization attacks but at the same time watermark extraction performance for JPEG compression deteriorates.

## REFERENCES

- [1]. Bender, W., Gruhl, D., Morimoto, N., and Lu, A. “Techniques for Data Hiding”, IBM Systems Journal, Vol. 35, Nos. 3&4, pp. 313-336, 1996.
- [2]. Pitas, I. “A Method of Signature Casting on Digital Images” Proceedings of IEEE International Conference on Image Processing, ICIP-1996, Vol.3, pp. 215-218, 1996.
- [3]. Wong, P. W. “A Public Key Watermark for Image Verification and Authentication”, Proceedings of IEEE International Conference on Image Processing, Chicago, Illinois, USA, Vol. 1, pp. 425-429, October 1998.
- [4]. Wolfgang, R. B., and Delp, E. J. “A Watermark for Digital Images”, Proceedings of International Conference on Image Processing, Vol. 3, pp. 219-222, Sept.1996.
- [5]. Schyndel, R. G., Tirkel, A., and Osborne, C. F. “A Digital Watermark”, Proceedings of IEEE International Conference on Image Processing, ICIP-1994, pp. 86-90, 1994.
- [6]. Kitamytra, Kanai, S., Kanai, T., and Kishinami, T. “Copyright Protection of Vector Map using Digital Watermarking Method based on Discrete Fourier Transform”, Proceedings of IEEE International Symposium on Geosciences and Remote Sensing, pp.1191-1193, 2001.
- [7]. Solachidis, V., and Pitas, I. “Circularly Symmetric Watermark Embedding in 2D-DFT domain”, IEEE Transactions on Image Processing, Vol. 10, No. 11, pp. 1741-1753, Nov. 2001.

- [8]. Hernandez, J. R., Amado, M., and Gonzalez, F.P. "DCT-Domain Watermarking Techniques for Still Images Detector Performance Analysis and a New Structure", *IEEE Transactions on Image Processing*, Vol. 9, No. 1, pp. 55-68, Jan. 2000.
- [9]. Barni, M., Bartolini, F., Cappellini, V., and Piva, A. "A DCT Domain System for Robust Image Watermarking", *Signal Processing (Special Issue on Watermarking)*, Vol. 66, No. 3, pp. 357-372, May 1998.
- [10].Lai, C. C., and Tsai, C.C., "Digital Image Watermarking Using Discrete Wavelet Transform and Singular Value Decomposition", *IEEE Transaction on Instrumentation and Measurement*, Vol. 59, No. 11, pp.3060-3063, Nov. 2008.
- [11].Yaw Low, C., Jin Teoh, A. B., and Tee, C. "Fusion of LSB and DWT Biometric Watermarking for Offline Handwritten Signature", *Proceedings of Congress on Image and Signal Processing, CISP'08*, Vol. 5, pp. 702-708, May 2008.
- [12].Haj, A. A., and Abu-Errub, A. "Performance Optimization of Discrete Wavelet Transform Based Image Watermarking using Genetic Algorithms", *Journal of Computer Science*, Vol. 4, No. 10, 2008.
- [13].Safabakhsh, R., Zabolli, S., and Tabibiazar, A. "Digital Watermarking on Still Images using Wavelet Transform" *Proc. of International Conference on Information Technology: Coding and Computing- ITCC-2004*.
- [14].Djurovic, I., Stankovic, S., and Pitas, I. "Digital Watermarking in the Fractional Fourier Transformation Domain", *Journal of Network and Computer Applications*, Vol. 24, No. 4, pp. 167-173, July 2001.
- [15].Yu, F.Q., Zhang, Z. K., and Xu, M. H. "A Digital Watermarking Algorithm for Image Based on Fractional Fourier Transform", *Proceedings of 1st IEEE International Conference on Industrial Electronics and Applications, ICIEA 2006*, pp. 1-5, 2006.
- [16].Hong, W. D., Ming, L. D., Jun, Y., and Xiong, C. F. "An Improved Chirp Typed Blind Watermarking Algorithm Based on Wavelet and Fractional Fourier Transform", *Proceedings of IEEE International Conference on Images and Graphics, ICIG 2007*, pp. 291-296, 22-24 Aug. 2007.
- [17].Feng, Z., Xiaomin, M. U., and Shouyi, Y. "Multiple Chirp Typed Blind Watermarking Algorithm Based on Fractional Fourier Transform", *Proceedings of International Symposium on Intelligent Signal Processing and Communication Systems, ISPACS 2005*, pp. 141-144, 13-16 Dec. 2005.
- [18].Kothari, A. M., Suthar, A. C., and Gajre, R. S. "Performance Analysis of Digital Image Watermarking Technique- Combined DWT- DCT over individual DWT", *International Journal of Advanced Engineering & Applications*, Jan. 2010.
- [19]. Haj, A. A. "Combined DWT-DCT Digital Image Watermarking", *Journal of Computer Science*, Vol. 3, No. 9, pp. 740-746, Sept. 2007.
- [20]. Abdulfetah, A. A., Sun, X., Yang, H., and Mohammad, N. "Robust Adaptive Image Watermarking using Visual Models in DWT and DCT domain", *Information Technology Journal*, Vol. 9, No. 3, pp. 460-466, 2010.
- [21]. Kang, X., Huang, J., Shi, Y. Q., and Lin, Y. "A DWT-DFT Composite Watermarking Scheme Robust to Both Affine Transform and JPEG Compression", *IEEE Transactions on Circuits and Systems for Video Technology*, Vol. 13, No. 8, pp. 776-786, August, 2003.
- [22].Mallat, S. G. "A Theory for Multiresolution Signal Decomposition: The Wavelet Representation", *IEEE Transactions on Pattern Analysis and Machine Intelligence*, Vol. 11, No. 7, pp. 674-693, July 1989.
- [23].Addison, P. "The Little Wave with the Big Future", *Physics World*, Vol. 17, pp. 35-39, March 2004.
- [24].Soman, K. P., Ramachandran, K. I. "Insight into Wavelets: From Theory to Practice", 2nd Edition, Prentice Hall of India, 2004.
- [25].Ozaktas, H. M., Arikan, O., Kutty, O., and Bazardag, M. A. "Digital Computation of the Fractional Fourier Transform", *IEEE Transactions on Signal Processing*, Vol. 44, No. 9 pp. 2141-2150, September 1996.
- [26].Kundur, D., and Hatzinakos, D. "A Robust Digital Image Watermarking Method using Wavelet Based Fusion", *Proceedings of IEEE International Conference on Image Processing, ICIP 1997*, Vol. 1, pp. 544-547, 1997.

Table 1: Performance comparison of three watermark methods in terms of BER under different attacks for ‘Lena’ Image

Attacks	DWT Method	DFRFT Method	Proposed Method: Combined DWT and DFRFT method											
			Sub-bands in DWT											
			LH2	HL2	HH2	LH1 + HL1	HL1 + HH1	LH1 + HH1	LH2 + HL2	HL2 + HH2	LH2 + HH2	LH1 + LH2	HL1 + HL2	HH1 + HH2
Salt & Peppers Noise	32.15	12.51	12.99	14.94	11.43	12.01	11.13	11.33	13.57	12.21	12.11	10.74	11.04	11.43
Median Filtering (3x3)	17.76	4.49	10.45	10.45	10.45	10.45	10.45	10.45	10.45	10.45	10.45	10.45	10.45	10.45
AWGN	12.29	3.8	5.37	4.4	4.4	5.18	4.69	4.3	5.08	3.61	4.49	3.52	4.0	4.0
JPEG Compression (QF=70)	8.26	4.1	10.16	10.06	10.45	10.45	10.45	10.45	10.35	10.45	10.45	10.45	10.45	10.45
Low-Pass Filtering	23.31	17.29	11.33	10.65	10.45	10.55	10.45	10.65	10.84	10.55	10.65	10.84	10.45	10.45
Histogram Equalization	45.49	88.48	1.27	2.25	0.68	0.0	0.0	0.0	0.98	0.59	0.29	0.098	0.098	0.098
Sharpening	35.1	74.81	3.61	3.91	1.27	0.0	0.0	0.0	2.54	0.88	1.07	0.098	0.098	0.098

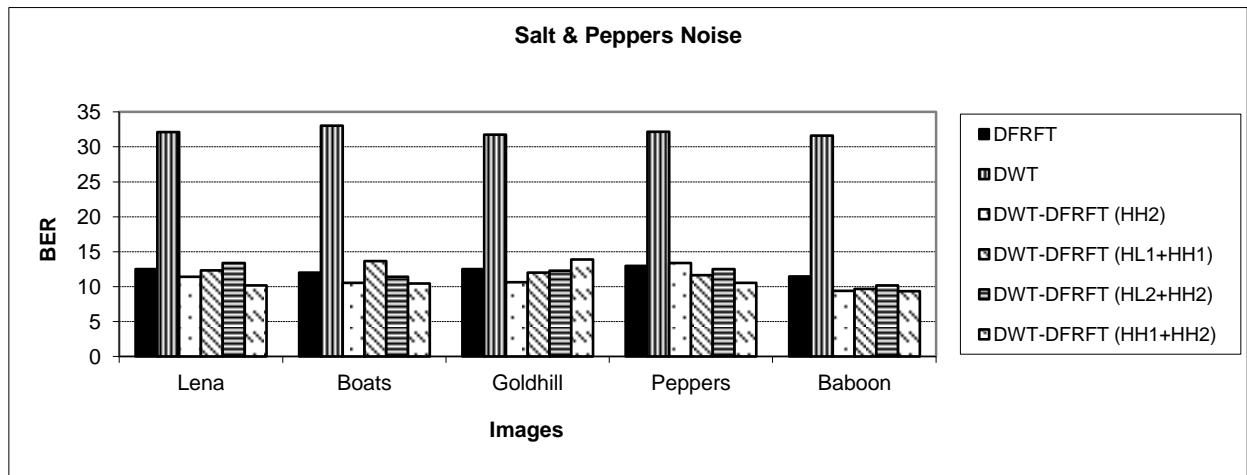


Figure 5 Effect of Salt & Peppers Noise on Watermark Extraction.

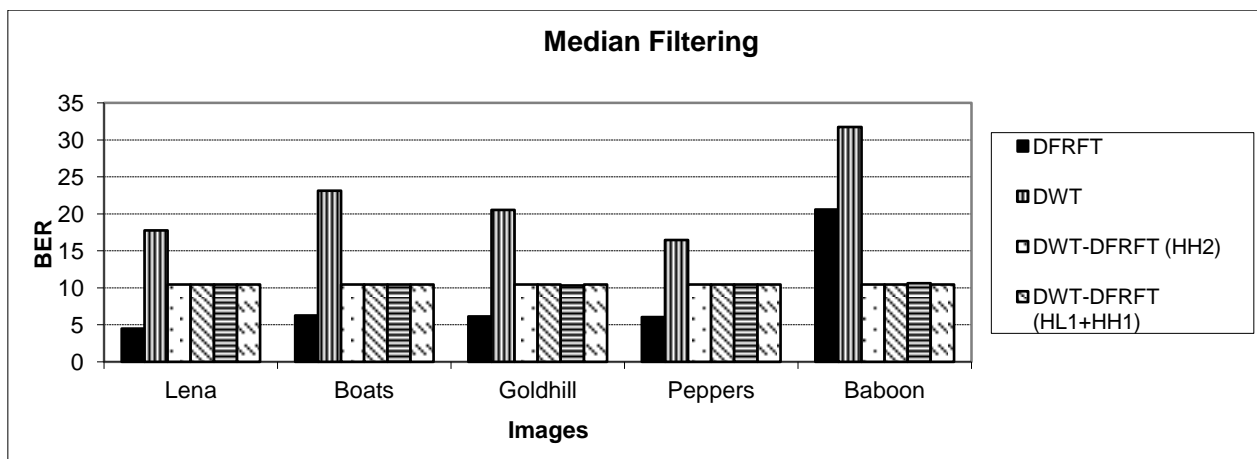


Figure 6 Effect of Median Filtering on Watermark Extraction.

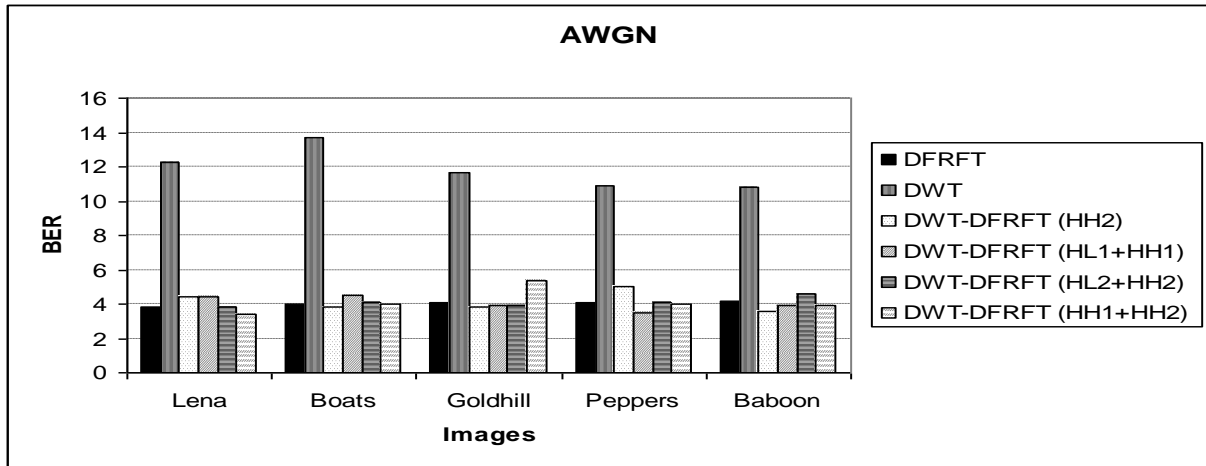


Figure 7 Effect of AWGN on Watermark Extraction.

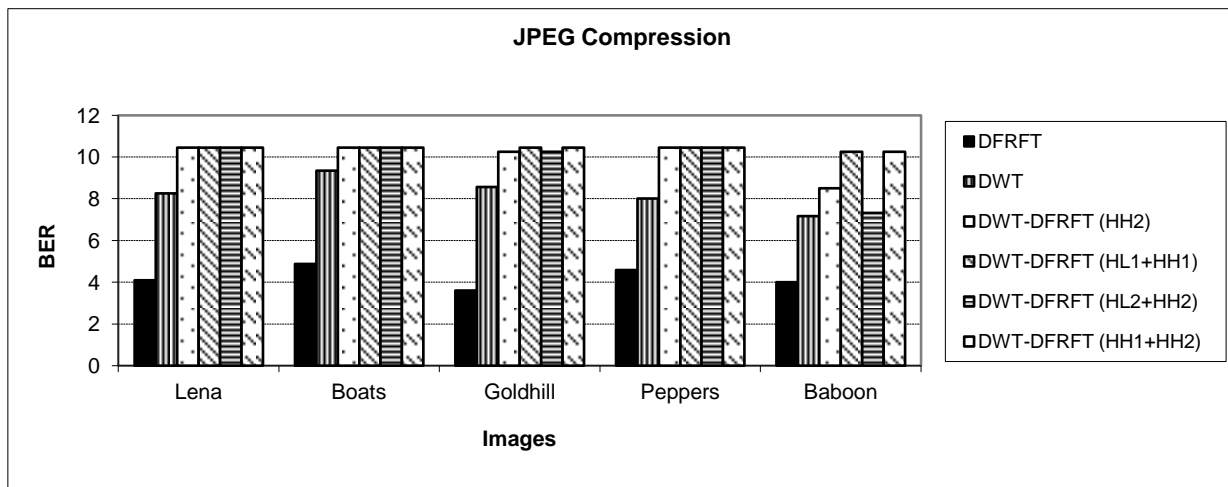


Figure 8 Effect of JPEG Compression (QF = 70%) on Watermark Extraction.

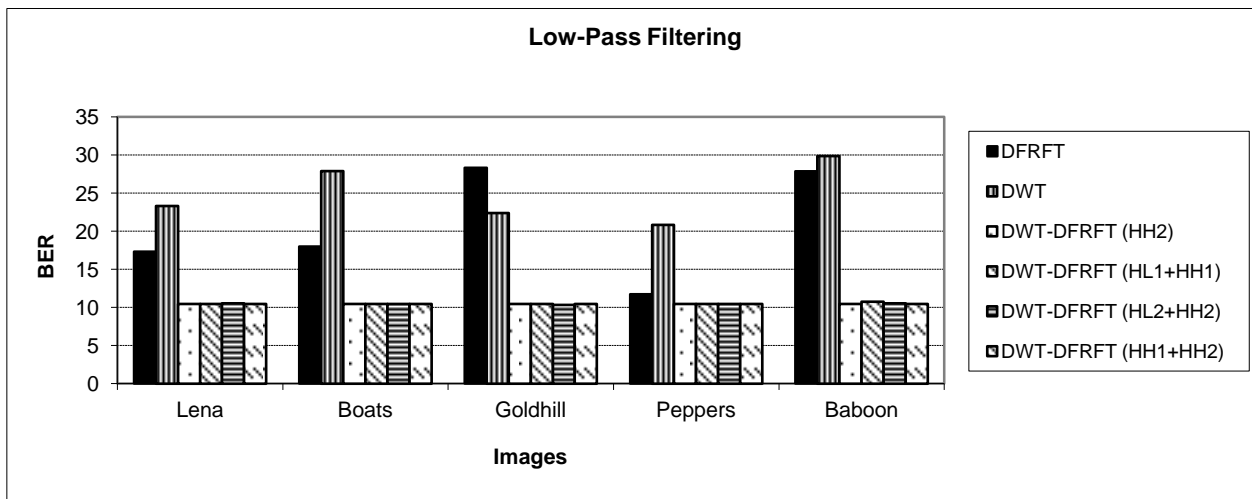


Figure 9 Effect of Low-Pass Filtering on Watermark Extraction.

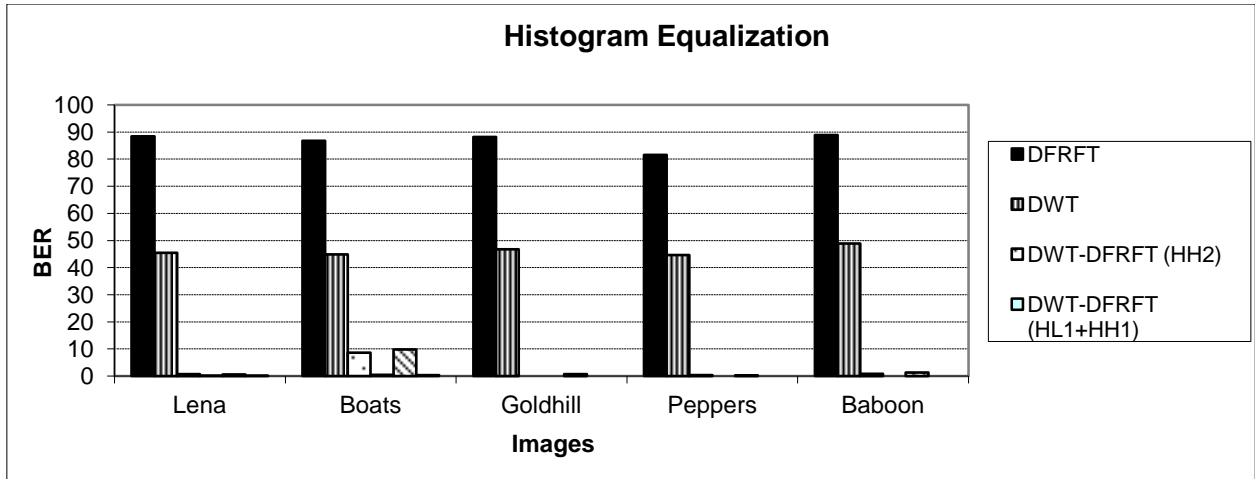


Figure 10 Effect of Histogram Equalization on Watermark Extraction.

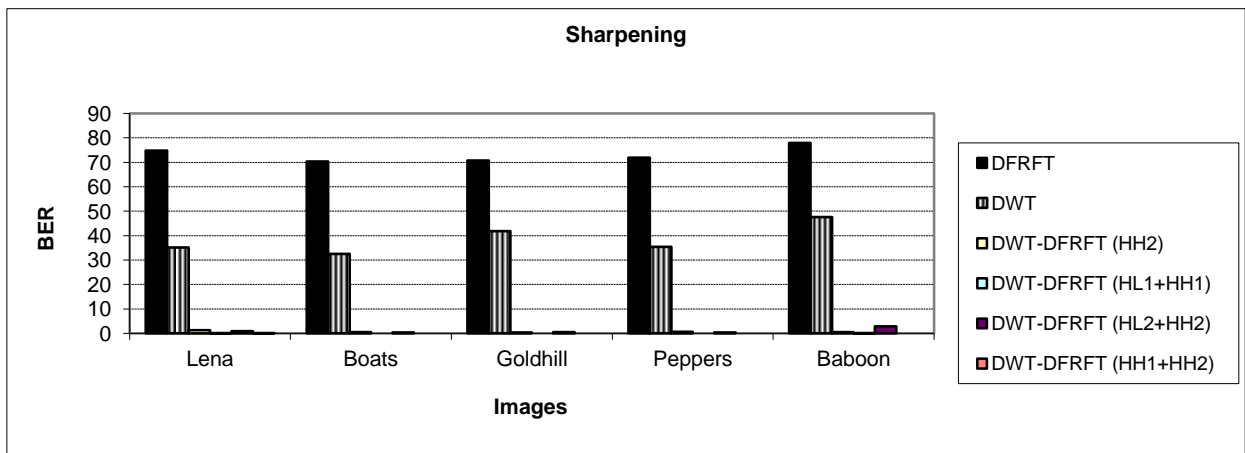


Figure 11 Effect of Sharpening on Watermark Extraction.